PROCESS MODELLING APPLIED TO FRICTION STIR WELDING OF Al-Mg-Si ALLOYS

By

Ø. Frigaard*, B. Bjørneklett*, Ø. Grong* and O.T. Midling**

* Norwegian University of Science and Technology, Department of Metallurgy, N-7032 Trondheim, Norway.
** Hydro Aluminium AS, R&D Materials Technology, N-4265 Håvik, Norway.

ABSTRACT

In the present investigation a 3-D numerical heat flow model for friction stir welding (FSW) of aluminium alloys has been developed, based on the finite difference approach. The algorithm is implemented in MatLab 5.1 and coupled with a dedicated microstructure model for AA 6082-T6 alloys to predict the resulting HAZ hardness. The simulations reveal a direct relationship between the thermal programme and the minimum HAZ strength level. This means that the potential of FSW cannot be fully utilised in engineering design, unless the heat generation is reduced to minimise the strength loss within the weld HAZ.

Keywords: *Aluminium, Friction stir welding, Modelling, Heat flow phenomena, Microstructure evolution.*

1. INTRODUCTION

The interest in friction stir welding (FSW) has gained considerable momentum over the past few years [1]. This is because the process has made it possible to implement the advantage of solid state bonding to plate and profile joints, thus leading to new product design previously not feasible [2]. In FSW the heat is generated by rotating movement of the shoulder and the pin. The frictional heating contributes to the formation of a plasticized layer of soft metal beneath the tool shoulder and about the pin. The material is then transported to the flow side of the tool due to the imposed mechanical stirring and forging action before it cools and forms a solid state joint [3].

In recent years, significant progress has been made in the understanding of physical processes that take place during welding of aluminium alloys. A synthesis of that knowledge has, in turn, been consolidated into process models, which provide a mathematical description of the relation between the main welding variables (e.g. heat input, plate thickness, joint configuration etc.) and the resulting weld properties, based on sound physical principles [4,5]. The components of such a model will be:

(i) A heat flow model for prediction of the temperature-time pattern during welding.
(ii) Kinetic models for prediction of the HAZ microstructure evolution (e.g. volume fraction of hardening precipitates) as a function of temperature.
(iii) Constitutive equations, based on dislocation mechanics, which provide quantitative information about the resulting heat affected zone (HAZ) hardness or strength.

In the present investigation, this concept is further developed and applied to friction stir welding of AA 6082-T6 aluminium alloys.

2. COMPONENTS OF THE MODEL

In the following, the components of the process model will be briefly described.

2.1 Heat Flow Model

An estimate of the heat generation during FSW can be obtained by considering the torque required to rotate a circular shaft relative to the plate surface under the action of an axial load [6]:

$$M = \int_0^{M_R} dM = \int_0^{R} \mu P(r) 2\pi r^2 dr = \frac{2}{3}\mu\pi P R^3 \qquad (1)$$

where M is the interfacial torque, μ is the friction coefficient, R is the surface radius, and $P(r)$ is the pressure distribution across the interface (here assumed constant and equal to P [Pa]). If all the shearing work at the interface is converted into frictional heat, the average heat input per unit area and time becomes [7]:

$$q_0 = \int_0^{M_R} \omega \, dM = \int_0^{R} \omega 2\pi\mu P r^2 dr = \frac{4}{3}\pi\mu P N R^3 \qquad (2)$$

where q_0 is the net power (in [W]),$\omega=2\pi N$ is the angular velocity (in [rad/s]), and N is the rotational speed [rot/s].

When the heat generation is known, numerical methods can be employed to calculate the resulting HAZ temperature distribution. The 3-D heat flow model adapted in the present investigation is based on a finite difference analogy of Fourier's second law for non-steady heat conduction in solids [8]:

$$\frac{\partial T}{\partial t} = a\left(\frac{\partial^2 T}{\partial x^2} + \frac{\partial^2 T}{\partial y^2} + \frac{\partial^2 T}{\partial z^2}\right) \qquad (3)$$

The algorithm is implemented in MatLab 5.1,which makes the model flexible and accessible to potential industry users. At the same time separate post-processing routines have been developed in order to present the outputs from the computations graphically. Details are given in Ref.[9,10].

2.2 Microstructure Model

During welding of AA 6082-T6 alloys reversion of β''-precipitates will occur to an increasing extend in the peak temperature range from 250 to 500°C. This is associated with a continuos decrease in the HAZ hardness until the dissolution process is completed. During cooling of the weld, some solute recombines to form coarse, metastable β'(Mg_2Si) precipitates which do not contribute to strengthening. However, close to the fusion boundary a large fraction of alloying elements will remain in solid solution at the end of the thermal cycle, thereby giving conditions for extensive age-hardening at room temperature over a period of 5-7 days.

Reversion model

If the number of particles per unit volume is constant, and the particle volume fraction f and radius r do not vary independently, reversion can be described by a single state variable f. Under such conditions simple diffusion theory shows that the volume fraction falls from its initial value f_i according to the equation [11,5]:

$$\frac{f}{f_0} = 1 - \left(\int dt/t_1^*\right)^{n_1} \quad (4)$$

where n_1 is a time exponent (<0.5), and t_1^* is the time taken for complete particle dissolution at a given temperature (defined in Refs.[5,11]). Because this equation satisfies the additivity conditions pertaining to an isokinetic reaction it can be integrated numerically over the actual weld thermal cycle in any position within the HAZ.

Natural ageing model

By considering the form of the C-curve for precipitation of non-hardening β'(Mg_2Si) precipitates at dispersoids, coupled with an analysis of the natural ageing kinetics, Myhr and Grong [11] arrived at the following expression for the net precipitation increment, referred to the initial content of hardening phases in the peak aged base material:

$$\frac{f}{f_0} = \Phi\left[(1 - X_c)^{I_1} - \alpha_1\right]^2 \quad (5)$$

where

$$I_1 = \left[\int dt/t_2^*\right]^{n_2} \quad (6)$$

Here Φ is a proportionality constant, while t_2^* denotes the time taken to precipitate a certain fraction ($X=X_c$) of β'at an arbitrary temperature T. The variation of t_2^* with temperature is given in Refs.[11,12].

Response equation

The strength of 6XXX-alloys is primarily determined by the density and size of the hardening β''-(Mg_2Si) precipitates. In the model, the local strength level is calculated via the following response equation which is based on simple dislocation theory [4,11]:

$$\alpha = (HV - HV_{min})/(HV_{max} - HV_{min}) = f/f_0 \quad (7)$$

Here HV_{min} denotes the intrinsic matrix strength after complete particle dissolution, while HV_{max} is the original base metal strength in the T6 temper condition.

3. CASE STUDIES

In the following, three different case studies will be presented to illustrate the basic features of the process model and how the final properties achieved depend on the HAZ temperature distribution. Table 1 contains a summary of welding parameters used in the modelling exercises.

Table 1. Summary of welding parameters used in modelling exercises.

Case No.	T_{max}* [°C]	plate width [mm]	plate length [mm]	d [mm]	v [mm/s]	R [mm]	μ	q_0 [W]
case 1	550	100	150	6	5	8	0.5	800
case2	550	100	150	6	8	8	0.5	800
case3	550	100	150	6	12.5	8	0.5	800

*Assumed maximum temperature beneath the tool shoulder.

3.1 HAZ hardness distributions

Based on the process model presented in the preceding sections, it is possible to construct two-dimensional maps which show characteristic isothermal and hardness contours in the HAZ. Examples of such diagrams are given in Figure 1 through Figure 3 for the combination of parameters listed in Table 1. In general, the results are in good agreement with experimental observations.

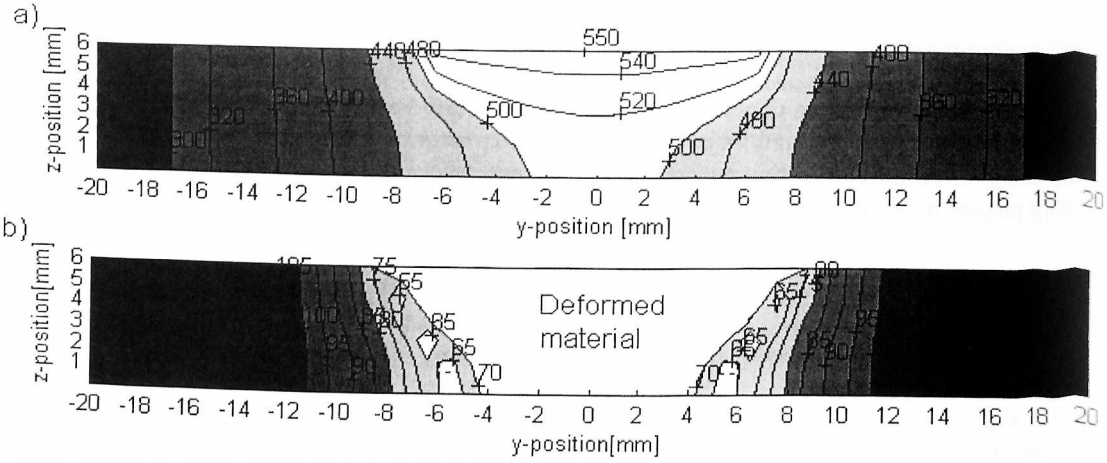

Figure 1a) Computed peak temperature contours in the cross section of the weld at pseudo-steady state b) Resulting HAZ hardness distribution following natural ageing [HV]; operating conditions as in Table 1 (case 1).

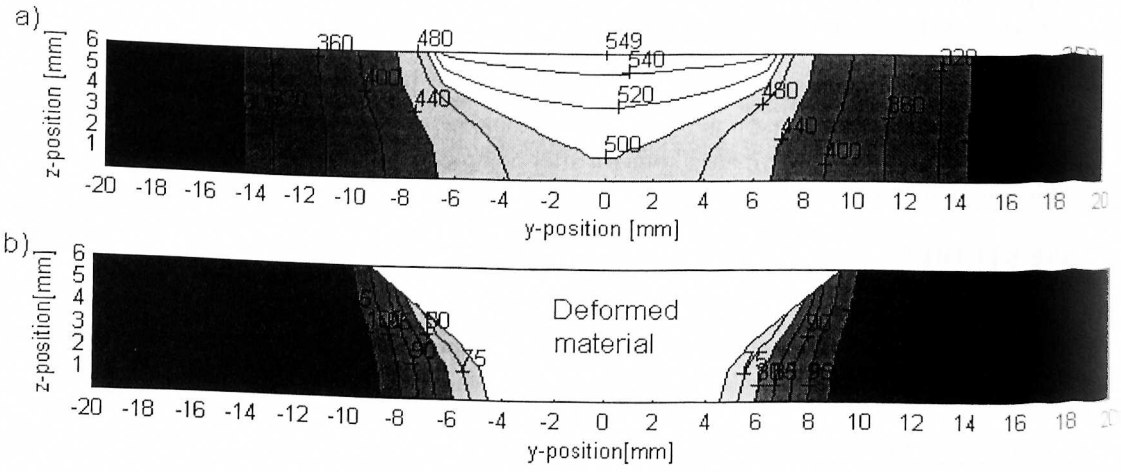

Figure 2a) Computed peak temperature contours in the cross section of the weld at pseudo-steady state b) Resulting HAZ hardness distribution following natural ageing [HV]; operating conditions as in Table 1 (case 2).

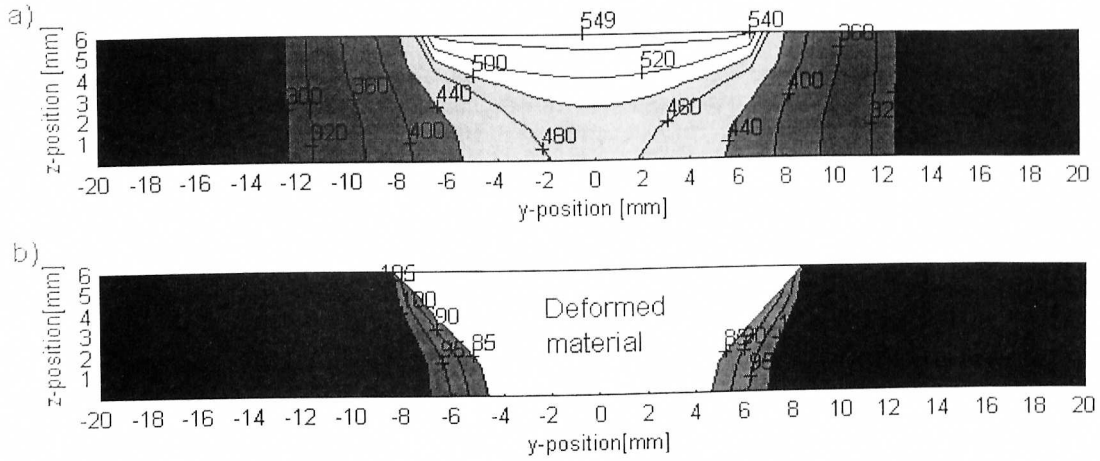

Figure 3a) Computed peak temperature contours in the cross section of the weld at pseudo-steady state b) Resulting HAZ hardness distribution following natural ageing [HV]; operating conditions as in Table 1 (case 3).

A closer inspection of the figures reveals a direct relationship between the HAZ thermal programme and the resulting hardness distribution following natural ageing. In general, a narrow width of the HAZ requires the use of a low energy input per unit area of the weld (i.e. a small q_0/vd ratio). As shown in Figure 3, the softest parts of the HAZ fall within the fully plasticized region of the weld when the travel speed is 12.5 mm/s. Under such conditions, the contribution from dislocation strengthening due to work hardening will tend to override the corresponding thermal softening of the base material. This observation is in sharp contrast to the results in Figure 1 and Figure 2, where parts of the soft zone are located outside the fully plasticized region of the weld. In the latter case, the predicted HAZ hardness profiles closely resemble those observed during conventional arc welding of AA6082-T6 alloys [4,11]. This means that the potential of FSW cannot be fully utilised in engineering design, unless the heat generation is reduced to minimise the strength loss within the weld HAZ.

Attempts are currently being made to develop a separate strength model for the fully plasticized region beneath the tool shoulder. This model will have roots in dislocation mechanics and hot deformation theory to ensure a high degree of predictive power.

4. ACKNOWLEDGEMENTS

The authors acknowledge the financial support from the Norwegian Research Council and Hydro Aluminium R&D Materials Technology.

5. REFERENCES

1. C. J. Dawes and W. M. Thomas, Welding Journal, 1996, vol. 75, No. 3, 41-45.
2. O.T. Midling and H.G. Johansen, Presentation at the 6th International Aluminium Technology Seminar & Exposition, ET96, Chicago, Illinois14.-17. May 1996.
3. O.T. Midling, Proceedings of the Aluminium 97 Conference, 24.-25. September 1997, Essen, Germany.
4. Ø. Grong, Metallurgical Modelling of Welding, Second Edition, The Institute of Materials, London, 1997.
5. O.R. Myhr, Ø. Grong, S. Klokkehaug, H.G. Fjær and A.O. Kluken: Sci. Techn. Weld. Join., 1997, vol.2, pp.245-253.
6. B. Crossland, Friction Welding, Cont. Phys., 1971, vol.12, (6), pp. 559-574.
7. Kong, H.S. and Ashby M.F., Case studies in the application of temperature maps for dry sliding, Engineering Dept. report, Cambridge University, 1991, pp. 4.
8. H.S. Carslaw and J.C. Jaeger: Conduction of Heat in Solids; 1959, Oxford, Oxford University Press.
9 Ø. Frigaard, SINTEF Report: STF24 A97625, Trondheim, Norway.
10 Ø. Frigaard, Ø. Grong and O.T. Midling, Modelling of heat flow phenomena in friction stir welding of aluminium alloys, Proc. 7th Int. Confr. in Joints in Aluminium (INALCO'98), TWI, Abington, Cambridge, UK, 15-17 April 1998.
11. O.R. Myhr and Ø. Grong: Acta Metall. Mater., 1991, vol 39, 2693-2702; ibid.,2703-2708.
12 D.H. Bratland, Ø. Grong, H.R. Schercliff, O.R. Myhr and S. Tjøtta: Overview No. 124 Acta Mater., 1997, vol 45, 1-22.